
Determination of Skeletal Tumor Burden on ^{18}F -Fluoride PET/CT

Eric M. Rohren¹, Elba C. Etchebehere^{1,2}, John C. Araujo³, Brian P. Hobbs⁴, Nancy M. Swanston¹, Michael Everding¹, Tracy Moody¹, and Homer A. Macapinlac¹

¹Department of Nuclear Medicine, University of Texas M.D. Anderson Cancer Center, Houston, Texas; ²Division of Nuclear Medicine, University of Campinas (UNICAMP), Campinas, Brazil; ³Department of Genitourinary Medical Oncology, University of Texas M.D. Anderson Cancer Center, Houston, Texas; and ⁴Department of Biostatistics, University of Texas M.D. Anderson Cancer Center, Houston, Texas

The purpose of this study was to define a method to assess skeletal tumor burden with ^{18}F -labeled sodium fluoride PET/CT (^{18}F -fluoride PET/CT) and evaluate the reproducibility of these measurements.

Methods: Ninety-eight consecutive patients (90 men; mean age \pm SD, 65.7 ± 14.2 y) underwent 158 ^{18}F -fluoride PET/CT scans for evaluation of skeletal metastatic disease. In order to determine the mean normal bone SUV, initially a 1-cm spheric volume of interest (VOI) was placed over 5 bone sites: T12, L5, sacrum, right iliac bone, and right femur. For each patient, the mean SUV_{max} for all sites was generated. Afterward, a threshold value of normal bone uptake was established. Subsequently, skeletal tumor burden was determined by generating volumetric data using a whole-body segmentation method. Any SUV_{max} below the normal threshold was excluded from analysis, as were VOIs not related to metastatic disease. Statistics for the remaining VOIs were then generated and defined as the skeletal metastatic tumor burden by 2 parameters: total lesion fluoride uptake above an SUV_{max} of 10 (TLF_{10}) and fluoride tumor volume above an SUV_{max} of 10 (FTV_{10}). TLF_{10} and FTV_{10} reproducibility was determined using 2 independent and experienced PET/CT interpreters analyzing a subset of 13 ^{18}F -fluoride PET/CT scans. **Results:** Mean (\pm SD) normal bone SUV_{max} was 6.62 ± 1.55 for T12, 6.11 ± 1.73 for L5, 4.59 ± 1.74 for sacrum, 5.39 ± 1.72 for right iliac bone, and 3.90 ± 1.57 for right femur. The mean normal SUV_{max} for all 543 sites was 5.32 ± 0.99 . On the basis of these values, an SUV_{max} threshold of 10 was chosen to exclude normal bone from the volumetric calculations. Semiautomated measurements of TLF_{10} and FTV_{10} exhibited high interobserver reproducibility, within $\pm 0.77\%$ and $\pm 3.62\%$ of the inter-observer average for TLF_{10} and FTV_{10} , respectively. **Conclusion:** Determination of skeletal tumor burden with ^{18}F -fluoride PET/CT is feasible and highly reproducible. Using an SUV_{max} threshold of 10 excludes nearly all normal bone activity from volumetric calculations.

Key Words: fluoride PET/CT; NaF PET/CT; prostate cancer; bone metastases; skeletal tumor burden

J Nucl Med 2015; 56:1507–1512

DOI: 10.2967/jnumed.115.156026

Radionuclide bone scanning is frequently used to determine the presence and extent of skeletal metastases in a variety of malignancies, such as prostate carcinoma and breast carcinoma. Often, bone scanning is performed in the setting of clinical indicators of bone metastases such as skeletal pain or elevated markers of bone turnover (e.g., alkaline phosphatase) (1). The standard technique for bone scanning uses $^{99\text{m}}\text{Tc}$ conjugated to a pharmaceutical compound with affinity to bone, such as medronate, imaged with planar scintigraphy or SPECT/CT.

An alternative to conventional bone imaging is PET/CT using ^{18}F -labeled sodium fluoride (^{18}F -fluoride PET/CT). Some studies suggest improved sensitivity and specificity for ^{18}F -fluoride PET/CT over conventional bone scintigraphy in the detection of skeletal metastases, but currently there are no generally accepted recommendations on the use of PET/CT over conventional bone imaging.

Beyond disease detection and tumor staging, there is a critical role for imaging in the prediction and determination of therapy response. Baseline imaging characteristics have been shown in some tumors to correlate with outcome, such as in non-small cell lung carcinoma, where the intensity of ^{18}F -FDG uptake on PET/CT is an independent predictor of overall survival (2). In other tumors, the degree of response as determined by imaging can predict overall response and long-term outcome (3). Furthermore, early interim imaging can, in some instances, predict eventual response, allowing for an early change in therapeutic regimen (4).

Although many of the studies correlating functional imaging with outcome apply ^{18}F -FDG PET/CT as a surrogate for tumor metabolism, not all tumors or tumor manifestations are amenable to metabolic assessment. In particular, skeletal metastases from prostate carcinoma show variable, and often low, uptake on ^{18}F -FDG PET/CT (5). In most men with osseous metastatic disease from prostate carcinoma, bone scanning better represents the extent of disease than ^{18}F -FDG PET/CT. Although sensitive for the detection of disease, conventional bone scintigraphy lacks the quantitative or semiquantitative capabilities of PET/CT.

It should be possible, using ^{18}F -fluoride PET/CT, to generate semiquantitative measures of skeletal tumor burden, as has initially been performed with ^{18}F -sodium fluoride on a dedicated PET/CT scanner in 5 patients undergoing ^{223}Ra (6). It should also be possible to take this a step further and evaluate such measures for their role in prognosis and response assessment. It has, in fact, been suggested that skeletal tumor burden may be an important prognostic factor in patients undergoing systemic therapy (7).

Received Feb. 17, 2015; revision accepted Jun. 23, 2015.

For correspondence or reprints contact: Elba Etchebehere, Department of Nuclear Medicine, University of Texas M.D. Anderson Cancer Center, 1400 Pressler St., FCT 16.6005, Unit 1483, Houston, TX 77030 and Division of Nuclear Medicine, University of Campinas (UNICAMP), Rua Vital Brasil, 251, Campinas, Brasil, CEP 13083-888.

E-mail: elba.etcbehere@gmail.com

Published online Jul. 1, 2015.

COPYRIGHT © 2015 by the Society of Nuclear Medicine and Molecular Imaging, Inc.

The aim of this study was to propose a method for semiquantitative assessment of total skeletal tumor burden using ^{18}F -fluoride PET/CT, to evaluate the reproducibility of these measurements, and through examples to illustrate how these volumetric measures may be applied.

MATERIALS AND METHODS

This study was approved by the institutional review board (PA14-0848). Waivers of informed consent and authorization were granted for the retrospective analysis of the imaging data. Patients who underwent ^{18}F -fluoride PET/CT at our institution between January 1, 2013, and August 30, 2014, for evaluation of skeletal metastatic disease were studied. Ninety-eight consecutive patients (90 men and 8 women; mean age \pm SD, 65.7 ± 14.2 y) underwent 158 ^{18}F -fluoride PET/CT scans for evaluation of skeletal metastatic disease. The primary malignancies included prostate carcinoma ($n = 68$), osteosarcoma ($n = 6$), medullary thyroid carcinoma ($n = 8$), and other malignancies ($n = 16$).

^{18}F -fluoride PET/CT Acquisition

^{18}F -fluoride PET/CT was performed according to a standard clinical protocol. Briefly, the patients were required to be well hydrated before imaging and were instructed to empty their bladder immediately before image acquisition. ^{18}F -fluoride PET/CT was performed after intravenous administration of an average (\pm SD) of $11,729 \pm 1,332$ MBq (317 ± 36 mCi) of ^{18}F -labeled sodium fluoride. The time from injection to imaging was 54.21 ± 8.03 min (range, 40–92 min). Images were acquired approximately 50–60 min after radiotracer injection, from the vertex of the skull to the feet, on an integrated PET/CT scanner. Whole-body unenhanced CT scans were used for attenuation correction. The images were reconstructed iteratively and displayed in 2.5-mm slices in the transverse, coronal, and sagittal planes.

Determination of Normal Bone Values on ^{18}F -Fluoride PET/CT

^{18}F -fluoride PET/CT studies were displayed and evaluated on a workstation (MIM Vista). Normal bone was defined as a region of skeleton exhibiting mild diffuse uptake, without any focal uptake and without anatomic abnormalities identified on the CT portion of the

scan. In order to determine the mean normal bone SUV, initially a 1.0-cm spheric volume of interest (VOI) was placed over sites of normal bone. The sites were the T12 vertebral body, L5 vertebral body, mid sacrum, right posterior iliac bone, and intertrochanteric right femur. If any of these sites was found to be abnormal (metastatic disease, fracture, prior surgery, degenerative changes) on the CT portion of the scan, an alternative measurement was obtained on any of the following sites: T11 vertebral body, L4 vertebral body, lower sacrum, left posterior iliac bone, or intertrochanteric left femur. If neither the primary site nor the secondary site was evaluable, the measurement of that specific abnormal site was excluded for that particular patient. A mean SUV_{max} for all evaluable sites was then generated for each patient.

Determination of Skeletal Tumor Burden on ^{18}F -Fluoride PET/CT

Skeletal tumor burden was determined by generating volumetric data using a whole-body segmentation method. A semiautomatic VOI was drawn on the whole-body image of each patient with caution to encompass all metastatic sites. After the whole-body VOI was drawn, the lower threshold for determination of a VOI was set at an SUV_{max} of 10 (according to the established threshold of normal bone uptake). In addition to excluding any uptake below that threshold, we undertook a careful image review to determine whether a lesion was benign or malignant. To exclude sites of elevated ^{18}F -fluoride uptake unrelated to metastatic disease, such as urine in the renal collecting system, degenerative disease, and healing fractures, we interpreted all images by evaluating ^{18}F -fluoride uptake on the PET portion and anatomy on the CT portion (Fig. 1).

Afterward, volumetric parameters of skeletal fluoride uptake were obtained from the statistics generated with the final volumetric extraction. Using an SUV_{max} threshold of 10, we determined skeletal tumor burden by calculating the fluoride tumor volume within the VOI (FTV_{10}) and the total lesion fluoride uptake as a product of mean $\text{SUV}_{\text{max}} \times \text{VOI}$ (TLF_{10}).

After defining the feasibility and reproducibility of this method, we applied ^{18}F -fluoride PET/CT skeletal tumor burden (TLF_{10} and FTV_{10}) to clinical ^{18}F -fluoride PET/CT scans of prostate cancer patients undergoing treatment with ^{223}Ra -dichloride (Xofigo; Bayer Healthcare Pharmaceuticals Inc.).

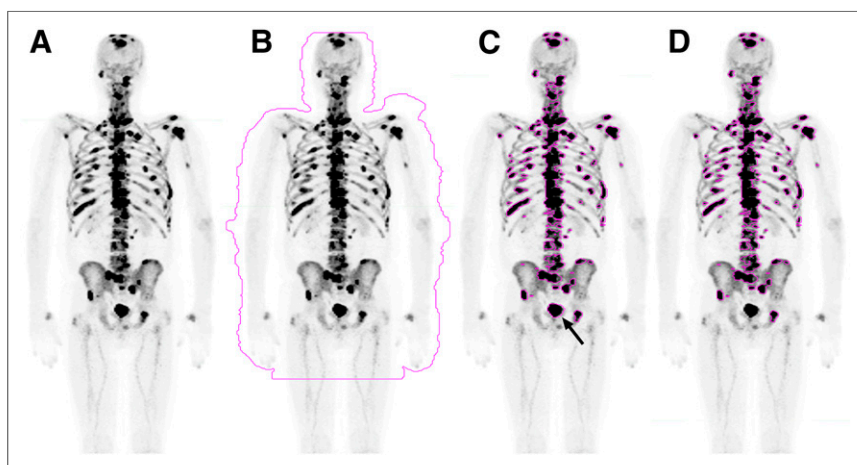


FIGURE 1. ^{18}F -fluoride PET/CT determination of skeletal tumor burden (TLF_{10} and FTV_{10}). (A) Whole-body ^{18}F -fluoride PET/CT image demonstrates widespread osteoblastic metastases. (B) Semiautomatic VOI contours whole-body image. (C) With SUV_{max} threshold of 10, all background activity within VOI is subtracted. The VOIs remaining delineate all metastatic sites but also delineate kidneys and bladder (arrow). (D) All nonmetastatic VOIs (bladder and kidneys) are then subtracted from the analysis.

Statistical Analysis

The Pearson product-moment correlation coefficient was used to measure the extent of linear dependence between mean bone SUV_{max} and age. The reproducibility of TLF_{10} and FTV_{10} was determined on a subset of 13 ^{18}F -fluoride PET/CT scans using 2 independent PET/CT interpreters, both of whom were board-certified nuclear medicine physicians with over 20 y of experience. Bland–Altman plots (8) are provided for both TLF_{10} and FTV_{10} , with corresponding 95% limits of agreement estimated using 1-way mixed-effects ANOVA. All plots and analyses were performed using the statistical software R (version 3.0; The R Foundation).

RESULTS

Normal Bone Values on ^{18}F -Fluoride PET/CT

In total, 158 ^{18}F -fluoride PET/CT scans of 98 patients were evaluated. Among the

TABLE 1
Results of Normal Bone SUV Measurements

SUV	T12	L5	Sacrum	R iliac bone	R femur
Minimum	2.12	2.07	1.69	2.39	1.12
Maximum	10.89	10.81	10.05	13.32	9.22
Median	6.69	6.13	4.23	5.29	3.72
Average	6.62	6.11	4.59	5.39	3.90
SD	1.55	1.73	1.74	1.72	1.57
Regions analyzed (of 543 total)	138	138	135	131	140

158 ^{18}F -fluoride PET/CT scans, 86 were acquired for staging and 72 to determine the subsequent treatment strategy (58 scans were acquired after the fourth ^{223}Ra dose, and 14 were acquired 3 mo after the last dose). Sixteen studies were not evaluable because of extensive metastatic disease and no measurable sites of normal bone (equivalent to a superscan). Therefore, normal bone SUV_{max} measurements were obtained from the remaining 142 ^{18}F -fluoride PET/CT scans, with a total of 543 sites assessed. The results of the normal bone SUV_{max} measurements are displayed in Table 1. No patient had more than 2 nonevaluable sites. The mean normal SUV_{max} for all 543 sites was 5.32 ± 0.99 . There was no relationship between the patient's mean bone SUV_{max} at the 5 measured sites and age ($R = -0.2464$, $R^2 = 0.0607$; Pearson correlation coefficient).

Skeletal Tumor Burden on ^{18}F -Fluoride PET/CT

Next, volumetric extraction of ^{18}F -fluoride PET/CT scans was undertaken. This necessitated the determination of a lower boundary below which fluoride activity would be excluded from analysis. The goal was to identify a threshold slightly above most normal bone to reliably exclude most normal osseous activity while including most sites of osseous metastatic disease. Using multiples of 5, we examined the database of normal bone SUV_{max} to determine how many of the normal bone sites would be erroneously included in the volumetric calculation. At a lower threshold of 5, 467 of 543 normal bone sites (86.0%) would be included in the VOI, whereas at a threshold of 10, only 6 of 543 (1.1%) would be included. On the basis of these results, an SUV_{max} threshold of 10 was chosen as the lower boundary for volumetric extraction to exclude most normal bone from the calculation of skeletal tumor burden.

Once the parameters had been determined, interinterpreter reproducibility of the technique was evaluated. Two experienced PET/CT interpreters independently performed volumetric whole-body extraction of ^{18}F -fluoride PET/CT scans with determination of TLF_{10} and FTV_{10} . Figure 2 summarizes the extent of observed interinterpreter agreement and depicts the estimated 95% agreement limits. Interinterpreter deviation was within $\pm 0.77\%$ of the interinterpreter average for TLF_{10} and within $\pm 3.62\%$ for FTV_{10} , demonstrating a high degree of interinterpreter reproducibility for the semiautomated measurements.

In addition, skeletal tumor burden (TLF_{10} and FTV_{10}) was quantified on baseline ^{18}F -fluoride PET/CT in a subset of 5 prostate cancer patients undergoing treatment with ^{223}Ra -dichloride. Figure 3 illustrates the difference in skeletal tumor burden values (TLF_{10}) in relation to prostate-specific antigen in responders and nonresponders to ^{223}Ra .

DISCUSSION

^{18}F -FDG PET/CT is an established biomarker to assess glycolytic tumor burden (9–17) in addition to being routinely performed for staging, restaging, evaluating treatment response, and predicting survival (18–21). However, not all tumors can be adequately evaluated with ^{18}F -FDG PET/CT. For many tumor types, bone scintigraphy plays an essential role through its ability to detect bone metastases, especially osteoblastic disease. However, assessment of disease extent and response on conventional bone scintigraphy has been challenging.

There is preliminary evidence that the more extensive the disease detected by scintigraphy, the worse the outcome (22,23). Initially, a 5-point grading system was developed to visually quantify skeletal tumor burden on bone scintigraphy (22); however, counting lesions is not practical. An objective means of quantifying skeletal tumor burden on bone scintigraphy was subsequently elaborated, although the quantification was manual and therefore not practical for routine use (24). Finally, a semiautomatic method was elaborated to quantify skeletal tumor burden on bone scintigraphy, which showed a correlation to survival (25).

Currently, with ^{18}F -fluoride PET/CT there is an even higher impact on patient management because it replaces the use of other imaging modalities such as body CT or MR imaging (26). Furthermore, when ^{18}F -fluoride is compared with $^{99\text{m}}\text{Tc}$ -medronate, the former has a higher uptake and blood clearance allowing faster PET/CT acquisitions and earlier imaging after radiotracer injection (15–30 min) (27,28). PET/CT has better spatial resolution

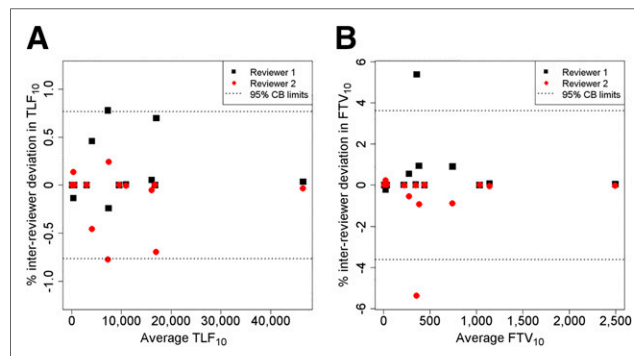


FIGURE 2. Bland-Altman plots for interinterpreter agreement in acquisition of TLF_{10} and FTV_{10} . Each plot depicts observed percentage deviation from interinterpreter mean in subsample of 13 patients assessed by 2 independent interpreters. The 95% limits of agreement obtained from 1-way mixed-effects ANOVA estimate extent of deviation from interinterpreter mean to be within $\pm 0.77\%$ for TLF_{10} and $\pm 3.62\%$ for FTV_{10} .

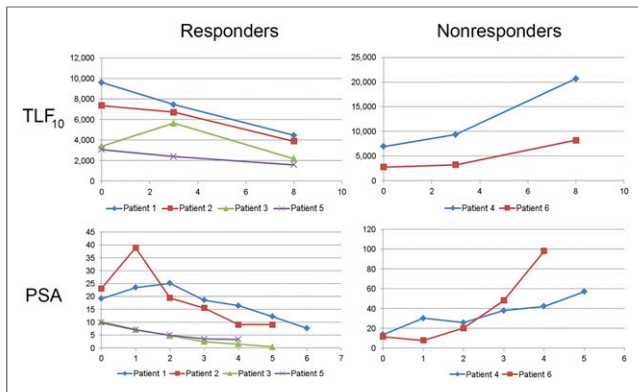


FIGURE 3. TLF₁₀ values and correlation to prostate-specific antigen (PSA) in responders and nonresponders to ²²³Ra.

than conventional scintigraphy, even when compared with SPECT/CT. For example, ¹⁸F-fluoride PET/CT is ideal for staging and restaging prostate cancer patients because of its greater sensitivity, specificity, and accuracy than conventional bone scintigraphy (29). Additionally, ¹⁸F-fluoride PET/CT has been of great value in defining equivocal bone metastases in prostate cancer patients when compared with bone scintigraphy (29–31).

To our knowledge, this was the first study to assess skeletal tumor burden using the intrinsic semiquantitative and volumetric nature of ¹⁸F-fluoride PET/CT. Through this work, we have defined several volumetric parameters of ¹⁸F-fluoride activity, includ-

ing total lesion ¹⁸F-fluoride uptake, which is analogous to total lesion glycolysis for ¹⁸F-FDG PET/CT, and ¹⁸F-fluoride tumor volume, which is analogous to metabolic tumor volume for ¹⁸F-FDG PET/CT. Other volumetric parameters can also be extracted, such as the mean ¹⁸F-fluoride activity of the total disease burden. Through the investigations described above, we have found that determination of these volumetric parameters from ¹⁸F-fluoride PET/CT is feasible and highly reproducible.

To calculate ¹⁸F-fluoride PET/CT skeletal tumor burden, it was important to establish the normal bone values. Prior ¹⁸F-fluoride PET/CT studies have demonstrated that SUV_{max} for normal bone is generally below 10 although the vertebral bodies may have a higher uptake (32). In our study, we found that 98.9% of normal bone at the 5 index sites had a mean SUV_{max} below 10. Therefore, an SUV_{max} of 10 excludes nearly all normal bone activity from volumetric calculations and skeletal tumor burden can easily be calculated and thus incorporated into a routine clinical setting. It is important to remember that although published reports have demonstrated SUV_{max} measurements above 10 for normal bone, none of our 198 scans had any sites of focal normal bone uptake above the established SUV_{max} of 10. One potential limitation of this study could have been the separation of benign abnormal findings (such as degenerative disease) from metastases. However, the CT portion of the scan helps overcome this limitation. Because we did not image patients at different time points, we cannot be sure if the uptake time distribution across our study population would affect the normal/metastasis values. We acquired our images within a shorter time than Sabbah et al. (54.21 ± 8.03 min vs. 76.5 ± 22.8 min), but they also

found a significant difference in SUV_{max} when normal bone was compared with metastases and did not find a significant number of metastases above an SUV_{max} of 10 (32). Kurdziel et al. (33) demonstrated that the SUV_{max} of metastases has a fairly stable plateau after a 30-min uptake period and that an SUV_{max} cutoff of 10 separates malignant from normal bone uptake. These high variations in acquisition time are likely in a busy clinical setting and should not invalidate our results.

Other thresholds could be used with this technique. In general, the lower the threshold for volumetric extraction, the higher the number of potential disease sites that will be included in the final parameters. However, this comes at a cost of including increasing amounts of normal bone in the final measurements. Raising the threshold (to, say, an SUV_{max} of 15 or 20) will diminish the potential for normal bone inclusion and may increasingly exclude sites of benign activity such as degenerative changes but will also progressively exclude sites of metastatic disease with low uptake. At this time, it is not clear which thresholds will provide optimal information for clinical decision making, and further studies will be needed. Although we provisionally suggest a threshold of 10 (generating TLF₁₀ and FTV₁₀) as a means to determine

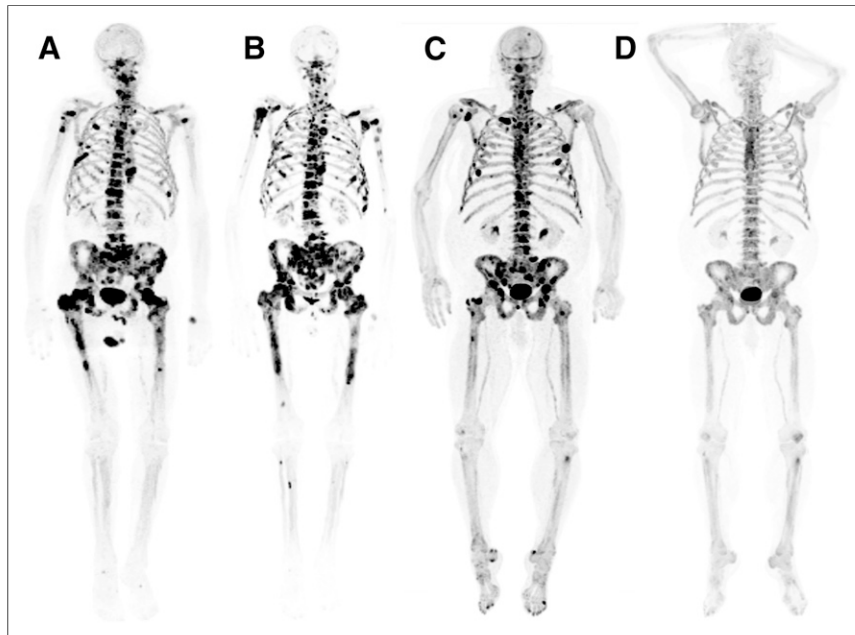


FIGURE 4. Patients with sequential ¹⁸F-fluoride PET/CT scans before and after treatment with ²²³Ra. (A) Patient's baseline ¹⁸F-fluoride PET/CT scan demonstrates widespread osteoblastic metastases with high ¹⁸F-fluoride uptake. Skeletal tumor burden was moderately increased (TLF₁₀, 2,729). (B) However, after treatment with ²²³Ra, patient had significant signs of progression, with additional sites of osteoblastic metastases. Skeletal tumor burden increased by 207% (TLF₁₀, 8,389). (C) Another example is this patient with baseline ¹⁸F-fluoride PET/CT also demonstrating widespread osteoblastic metastases with high uptake. Skeletal tumor burden was markedly increased (TLF₁₀, 5,576). (D) Fortunately, patient responded to treatment with ²²³Ra and skeletal tumor burden reduced 83.9% (TLF₁₀, 898).



FIGURE 5. ^{18}F -fluoride PET/CT scan with VOIs at established SUV_{max} threshold of 10. There is high ^{18}F -fluoride uptake on osteoblastic metastases. Once lesions are contoured on PET (A), CT (B), and fusion (C) images, it is easy to manually refine automatically generated thresholds and exclude sites of nonmalignant fluoride activity.

overall disease burden, higher thresholds (e.g., TLF_{50}) may also impart valuable information by differentiating areas of high bone turnover from areas of more quiescent disease.

Determining skeletal tumor burden with ^{18}F -fluoride PET/CT (TLF_{10} or FTV_{10}) may also help guide patient management. Figure 4 illustrates 2 patients with sequential ^{18}F -fluoride PET/CT scans before and after treatment with ^{223}Ra . The extraction and reporting of these semiquantitative metrics of ^{18}F -fluoride activity have the potential to shift the determination of overall skeletal tumor burden and assessment of therapy response beyond simple descriptors (e.g., “extensive disease” and “modest progression”) to a more defined and precise approach based on quantifiable values. The method used herein is semiautomated and fairly easy to perform. There is still a need for interpreter expertise, to manually refine the automatically generated thresholds and to manually exclude sites of nonmalignant fluoride activity, although refinements to the technique may allow for better automation in the future (Fig. 5).

Unlike prior investigations making use of conventional bone scintigraphy, the semiautomatic calculation was feasible, highly reproducible, and fast. A recent study, albeit with fewer patients, demonstrated the capacity of skeletal tumor burden to evaluate treatment outcome with dasatinib in prostate cancer patients (34). Further studies are needed to define the role of skeletal tumor burden before, during, or after therapy in other cancer types, such as breast cancer. In addition, it is important to evaluate the applicability of other statistical parameters (besides TLF_{10} and FTV_{10}) generated from the volumetric data that may have an impact on the posttherapeutic management of prostate cancer patients.

One limitation of this technique is that it measures only skeletal tumor burden, not all tumor burden. For diseases in which osteoblastic skeletal metastases predominate, the extent of ^{18}F -fluoride activity may be reasonably understood as a surrogate for overall disease extent. However, the underlying fate of tumor in response to therapy may not always be directly or linearly reflected in ^{18}F -fluoride uptake, such as in the commonly understood phenomenon of flare on bone scanning.

Although conventional bone scintigraphy shares these limitations, it still has a central role in the clinical management of select patient populations, but our study underscores the need for a full understanding of the physiology behind the imaging. A potential advantage of ^{18}F -fluoride PET/CT over conventional bone scintigraphy may be the availability of the concurrently acquired CT images, which may allow for detection and characterization of extraskeletal metastatic disease (including visceral disease) if the images are obtained using oral and intravenous contrast material.

Most patients analyzed in this study had advanced disease with known osseous metastases and, in many cases, extensive skeletal

involvement. We anticipate that the technique for determining TLF_{10} and FTV_{10} will be equally robust for the analysis of patients with a lower volume of disease. However, this technique does not in itself differentiate benign from malignant causes of fluoride uptake, and skillful visual analysis and interpretation of the images remain critical.

CONCLUSION

Volumetric parameters of ^{18}F -fluoride activity on PET/CT show tremendous potential for assessing total disease burden and therapy response in patients with predominantly osteoblastic skeletal metastases. Such measures have not been easily obtained using conventional bone scintigraphy but are relatively easy to extract and highly reproducible using ^{18}F -fluoride PET/CT. As with PERCIST, studies will be needed to determine whether such parameters impart valuable clinical information such as prognosis and outcome.

DISCLOSURE

The costs of publication of this article were defrayed in part by the payment of page charges. Therefore, and solely to indicate this fact, this article is hereby marked “advertisement” in accordance with 18 USC section 1734. This work was supported in part by the James E. Anderson Distinguished Professorship Endowment, an M.D. Anderson Cancer Center support grant from the National Cancer Institute (P30 CA016672), and FAPESP (Fundacao Amparo Pesquisa Estado de Sao Paulo). No other potential conflict of interest relevant to this article was reported.

REFERENCES

- Mohler JL, Kantoff PW, Armstrong AJ, et al. Prostate cancer, version 2.2014. *J Natl Compr Canc Netw*. 2014;12:686–718.
- Machtay M, Duan F, Siegel BA, et al. Prediction of survival by [^{18}F]fluorodeoxyglucose positron emission tomography in patients with locally advanced non-small-cell lung cancer undergoing definitive chemoradiation therapy: results of the ACIN 6668/RTOG 0235 trial. *J Clin Oncol*. 2013;31:3823–3830.
- Barber TW, Duong CP, Leong T, Bressel M, Drummond EG, Hicks RJ. ^{18}F -FDG PET/CT has a high impact on patient management and provides powerful prognostic stratification in the primary staging of esophageal cancer: a prospective study with mature survival data. *J Nucl Med*. 2012;53:864–871.
- Li YJ, Li ZM, Xia XY, et al. Prognostic value of interim and posttherapy ^{18}F -FDG PET/CT in patients with mature T-cell and natural killer cell lymphomas. *J Nucl Med*. 2013;54:507–515.
- Núñez R, Macapinlac HA, Yeung HW, et al. Combined ^{18}F -FDG and ^{11}C -methionine PET scans in patients with newly progressive metastatic prostate cancer. *J Nucl Med*. 2002;43:46–55.
- Cook G Jr, Parker C, Chua S, Johnson B, Aksnes AK, Lewington VJ. ^{18}F -fluoride PET: changes in uptake as a method to assess response in bone metastases from castrate-resistant prostate cancer patients treated with ^{223}Ra -chloride (Alpharadin). *EJNMMI Res*. 2011;1:4.
- Fizazi K, Massard C, Smith M, et al. Bone-related parameters are the main prognostic factors for overall survival in men with bone metastases from castration-resistant prostate cancer. *Eur Urol*. 2014;68:42–50.
- Bland JM, Altman DG. Statistical methods for assessing agreement between two methods of clinical measurement. *Lancet*. 1986;1:307–310.
- Zhang H, Wroblewski K, Pu Y. Prognostic value of tumor burden measurement using the number of tumors in non-surgical patients with non-small cell lung cancer. *Acta Radiol*. 2012;53:561–568.
- Zhang H, Wroblewski K, Liao S, et al. Prognostic value of metabolic tumor burden from ^{18}F -FDG PET in surgical patients with non-small-cell lung cancer. *Acad Radiol*. 2013;20:32–40.

11. Chen HHW, Chiu N-T, Su W-C, Guo H-R, Lee B-F. Prognostic value of whole-body total lesion glycolysis at pretreatment FDG PET/CT in non-small cell lung cancer. *Radiology*. 2012;264:559–566.
12. Kim MH, Lee JS, Mok JH, et al. Metabolic burden measured by ¹⁸F-fluorodeoxyglucose positron emission tomography/computed tomography is a prognostic factor in patients with small cell lung cancer. *Cancer Res Treat*. 2014;46:165–171.
13. Ezziddin S, Adler L, Sabet A, et al. Prognostic stratification of metastatic gastroenteropancreatic neuroendocrine neoplasms by ¹⁸F-FDG PET: feasibility of a metabolic grading system. *J Nucl Med*. 2014;55:1260–1266.
14. Kim CY, Hong CM, Kim DH, et al. Prognostic value of whole-body metabolic tumour volume and total lesion glycolysis measured on ¹⁸F-FDG PET/CT in patients with extranodal NK/T-cell lymphoma. *Eur J Nucl Med Mol Imaging*. 2013;40:1321–1329.
15. Fonti R, Larobina M, Del Vecchio S, et al. Metabolic tumor volume assessed by ¹⁸F-FDG PET/CT for the prediction of outcome in patients with multiple myeloma. *J Nucl Med*. 2012;53:1829–1835.
16. Klabatsa A, Chicklore S, Barrington SF, Goh V, Lang-Lazdunski L, Cook GJ. The association of ¹⁸F-FDG PET/CT parameters with survival in malignant pleural mesothelioma. *Eur J Nucl Med Mol Imaging*. 2014;41:276–282.
17. Basu S, Saboury B, Torigian DA, Alavi A. Current evidence base of FDG-PET/CT imaging in the clinical management of malignant pleural mesothelioma: emerging significance of image segmentation and global disease assessment. *Mol Imaging Biol*. 2011;13:801–811.
18. Furth C, Steffen IG, Amthauer H, et al. Early and late therapy response assessment with [¹⁸F]fluorodeoxyglucose positron emission tomography in pediatric Hodgkin's lymphoma: analysis of a prospective multicenter trial. *J Clin Oncol*. 2009;27:4385–4391.
19. Carkaci S, Sherman CT, Ozkan E, et al. ¹⁸F-FDG PET/CT predicts survival in patients with inflammatory breast cancer undergoing neoadjuvant chemotherapy. *Eur J Nucl Med Mol Imaging*. 2013;40:1809–1816.
20. Javeri H, Xiao L, Rohren E, et al. The higher the decrease in the standardized uptake value of positron emission tomography after chemoradiation, the better the survival of patients with gastroesophageal adenocarcinoma. *Cancer*. 2009;115:5184–5192.
21. Juweid ME, Wiseman GA, Vose JM, et al. Response assessment of aggressive non-Hodgkin's lymphoma by integrated International Workshop Criteria and fluorine-18-fluorodeoxyglucose positron emission tomography. *J Clin Oncol*. 2005;23:4652–4661.
22. Soloway MS, Hardeman SW, Hickey D, et al. Stratification of patients with metastatic prostate cancer based on extent of disease on initial bone scan. *Cancer*. 1988;61:195–202.
23. Sabbatini P, Larson SM, Kremer A, et al. Prognostic significance of extent of disease in bone in patients with androgen-independent prostate cancer. *J Clin Oncol*. 1999;17:948–957.
24. Imbriaco M, Larson SM, Yeung HW, et al. A new parameter for measuring metastatic bone involvement by prostate cancer: the Bone Scan Index. *Clin Cancer Res*. 1998;4:1765–1772.
25. Ulmert D, Kaboteh R, Fox JJ, et al. A novel automated platform for quantifying the extent of skeletal tumour involvement in prostate cancer patients using the Bone Scan Index. *Eur Urol*. 2012;62:78–84.
26. Hillner BE, Siegel BA, Hanna L, Duan F, Shields AF, Coleman RE. Impact of ¹⁸F-fluoride PET in patients with known prostate cancer: initial results from the National Oncologic PET Registry. *J Nucl Med*. 2014;55:574–581.
27. Blake GM, Park-Holohan SJ, Cook GJ, Fogelman I. Quantitative studies of bone with the use of ¹⁸F-fluoride and ^{99m}Tc-methylene diphosphonate. *Semin Nucl Med*. 2001;31:28–49.
28. Schiepers C, Nuyts J, Bormans G, et al. Fluoride kinetics of the axial skeleton measured in vivo with fluorine-18-fluoride PET. *J Nucl Med*. 1997;38:1970–1976.
29. Bortot DC, Amorim BJ, Oki GC, et al. ¹⁸F-fluoride-PET/CT is highly effective for excluding bone metastases even in patients with equivocal bone scintigraphy. *Eur J Nucl Med Mol Imaging*. 2012;39:1730–1736.
30. Even-Sapir E, Metser U, Mishani E, Lievshitz G, Lerman H, Leibovitch I. The detection of bone metastases in patients with high-risk prostate cancer: ^{99m}Tc-MDP planar bone scintigraphy, single- and multi-field-of-view SPECT, ¹⁸F-fluoride PET, and ¹⁸F-fluoride-PET/CT. *J Nucl Med*. 2006;47:287–297.
31. Schirrmester H, Guhlmann A, Elsner K, et al. Sensitivity in detecting osseous lesions depends on anatomic localization: planar bone scintigraphy versus ¹⁸F PET. *J Nucl Med*. 1999;40:1623–1629.
32. Sabbah N, Jackson T, Mosci C, et al. ¹⁸F-sodium fluoride PET/CT in oncology: an atlas of SUVs. *Clin Nucl Med*. 2015;40:e228–e231.
33. Kurdziel KA, Shih JH, Apolo AB, et al. The kinetics and reproducibility of ¹⁸F-sodium fluoride for oncology using current PET camera technology. *J Nucl Med*. 2012;53:1175–1184.
34. Yu EY, Duan F, Muzi M, et al. Castration-resistant prostate cancer bone metastasis response measured by ¹⁸F-fluoride PET after treatment with dasatinib and correlation with progression-free survival: results from American College of Radiology Imaging Network 6687. *J Nucl Med*. 2015;56:354–360.